Mathematical Simulation for Flood Inundation and Gate Operation of a Main Drainage Canal in a Flat Low-lying Agricultural Area

Le, Van Chinh
Graduate School of Bioresource and Bioenvironmental Sciences, Kyushu University

Hiramatsu, Kazuaki
Faculty of Agriculture, Kyushu University

Harada, Masayoshi
Faculty of Agriculture, Kyushu University

Mori, Makito
Faculty of Agriculture, Kyushu University

https://doi.org/10.5109/9331

出版情報：九州大学大学院農学研究院紀要. 52 (2), pp.411-422, 2007-10-29. Faculty of Agriculture, Kyushu University
バージョン：
権利関係：

J. Fac. Agr., Kyushu Univ., **52** (2), 411–422 (2007)

Mathematical Simulation for Flood Inundation and Gate Operation of a Main Drainage Canal in a Flat Low–lying Agricultural Area

Le Van CHINH[1]*, Kazuaki HIRAMATSU, Masayoshi HARADA and Makito MORI

Laboratory of Drainage and Water Environment, Division of Regional Environment Science,
Department of Bioproduction Environmental Sciences, Faculty of Agriculture,
Kyushu University, Fukuoka 812–8581, Japan
(*Received May 16, 2007 and accepted July 17, 2007*)

Chiyoda basin is located in Saga Prefecture in Kyushu Island, Japan, and lies next to the tidal compartment of the Chikugo River to which the excess water in the basin is drained away. Chiyoda basin has a total basin area of about 1,100 ha and is a typical flat and low–lying paddy–cultivated area. The main problem in this basin is the inundation analysis and prediction of the potential inundation in term of total inundation time, total inundation area, the coeficient of variances of maximum inundation depth in paddy tanks and the maximum inundation depth in paddy tanks. This paper presents a mathematical model of a drainage system in Chiyoda basin for calculating the flood inundation and predicting the potential inundation. First, the algorithm of gate operation was simulated and the drainage model was then evaluated by comparing the simulated water levels with observed ones during an actual rainfall event. The results show that the observed and simulated water levels are in good agreement, indicating that the proposed model is applicable for drainage and inundation analyses in flat low–lying paddy–cultivated areas. Second, the potential of inundation was predicted using a stochastic rainfall time series with a return period of 30 years and the tidal conditions of spring and neap tides in Chikugo River. The parameters of this inundation scenario such as a total inundation time, a total inundation area, a coefficient of maximum inundation depth in paddy tanks and maximum inundation depth in paddy tank were ditermined. For further, this model will be able to provide managers and operators a usefull tool that is to optimize the gate operation in order to minimize the damages for crop and store the water for the irrigation purposes.

Keywords: Flat low–lying paddy–cultivated area, flood inundation, irrigation requirement, tank model, check gate, optimal gate operation.

INTRODUCTION

During flood events, the drainage system in flat, low–lying, paddy–cultivated areas should require two functions: minimize the inundation damages to crop yield during the events, and store the water volume for irrigation purposes after the events. Therefore, it is necessary to simulate and analyze the inundation situation during flood events. Further more using the model to predict the potential inundation which corresponds with a return periods of rainfall and the tidal conditions of the boundary River.

Within the past few decades, the analysis of the rainfall–runoff process and simulation of flood inundation started from the use of a simple hydrological model such as a unit hydrograph to further the applications of complex hydrological models that combine transient flow theories. These models are widely used in the tasks of river controls, drainage planning and flood forecasting. Typical examples are the following works. Nicholas and Walling (1997) used a numerical model of flood hydraulics and overbank deposition on river floodplains for prediction of floodplain inundation squences, overbank deposition rates and deposit grain size distribution. Stewart *et al*. (1999) considered the modeling of lowland river in which content complex is reached with hydrological intersection. Bates and De Roo (2000) developed a simple raster–based model for flood inundation simulation. Hsu *et al*. (2000) simulated the inundation for urban drainage basin with a storm sewer system. Horritt and Bates (2001) applied a model for predicting floodplain inundation: raste–based modelling versus the finite–element approach. Pappenberger *et al*. (2005) used inundation and downstream water level observations to calibrate the effect of roughness parameters in HEC–RAS. Overton (2005) introduced a model of floodplain inundation on a regulated river by integrating GIS, remote sensing and a hydrological model. Dutta *et al*. (2006) presented an application of a flood risk analysis system for impact analysis of a flood control plan in a river basin.

To deal with all kinds of flow conditions, most of the hydrological models were constructed based on an unsteady flow approach. In flat, low–lying agricultural areas consisting of paddy fields and canals, tank models have been introduced for rainfall runoff analysis in order to overcome the model complexity and calculation time. For example, Shikasho and Tanaka (1984) executed the inundation analysis in a flat, low–lying paddy–cultivated area in Japan using a continuous tank model, and Chen *et al*. (2003) and Chen and Pi (2004) used a diffusive

[1] Laboratory of Drainage and Water Environment, Division of Regional Environment Science, Department of Bioproduction Environmental Sciences, Graduate School of Bioresource and Bioenvironmental Sciences, Kyushu University

* Corresponding author (E–mail: chinhhec1@bpes.kyushu–u.ac.jp)

tank model for rainfall–runoff analysis in local areas mixed with paddy and upland fields. Hiramatsu *et al.* (2004) applied a continuous tank model to simulate and analyze the inundation in a flat, low–lying paddy–cultivated area in the Red River delta in Vietnam. In these models, regional drainage systems were constructed by many interconnected tanks; therefore, the model can generally deal with every field and any kind of drainage and boundary conditions.

In terms of simulation of gate operation in agricultural canals, there has been much research. For example, Durdu (2006) applied an optimal fuzzy filter to solve the state estimation problem of the controlled irrigation canals. By using a linearized finite–difference model of the open–channel flow, Durdu formulated a canal operation problem as an optimal control problem and derived an algorithm for gate openings in the presence of unknown external disturbances. Ghumman *et al.* (2006) used numerical modeling to evaluate the performance of canal outlets under different discharge conditions and assessed the response of any modification in the dimensions of the canal outlets on water distribution. However, these researches dealt mainly with the gate operation that related to the irrigation scheduling and the irrigation water distribution. Few studies focused on the gate operation for both flood drainage and irrigation purposes. Chinh *et al.* (2005) applied a tank model incorporated with Genetic Algorithm to optimize the gate operation in a main drainage canal. However, Chinh *et a*l. dealt only with the optimization of the gate operation in order to avoid the local concentration of inundation during flood events.

In the present study, a continuous tank model for a typical flat and low–lying agricultural area in Japan was first constructed incorporated with the actual gate operation based on operators' experience. The water levels in a main drainage canal were then simulated using an observed rainfall time series in order to verify the predicted performance of the model. Next, the potential inundation was predicted using a stochastic rainfall time series with a return period of 30 years and the tidal conditions of spring and neap tides in Chikugo River.

MATERIALS AND METHODS

Study area

Chiyoda basin is located in Saga Prefecture in Kyushu Island, Japan. It is surrounded by the Jobaru River to the west and the Tade River to the east as shown in **Fig. 1**. It is a typical flat and low–lying agricultural area. The total basin area is about 1,100 ha, which is covered mostly by paddy fields. The excess water

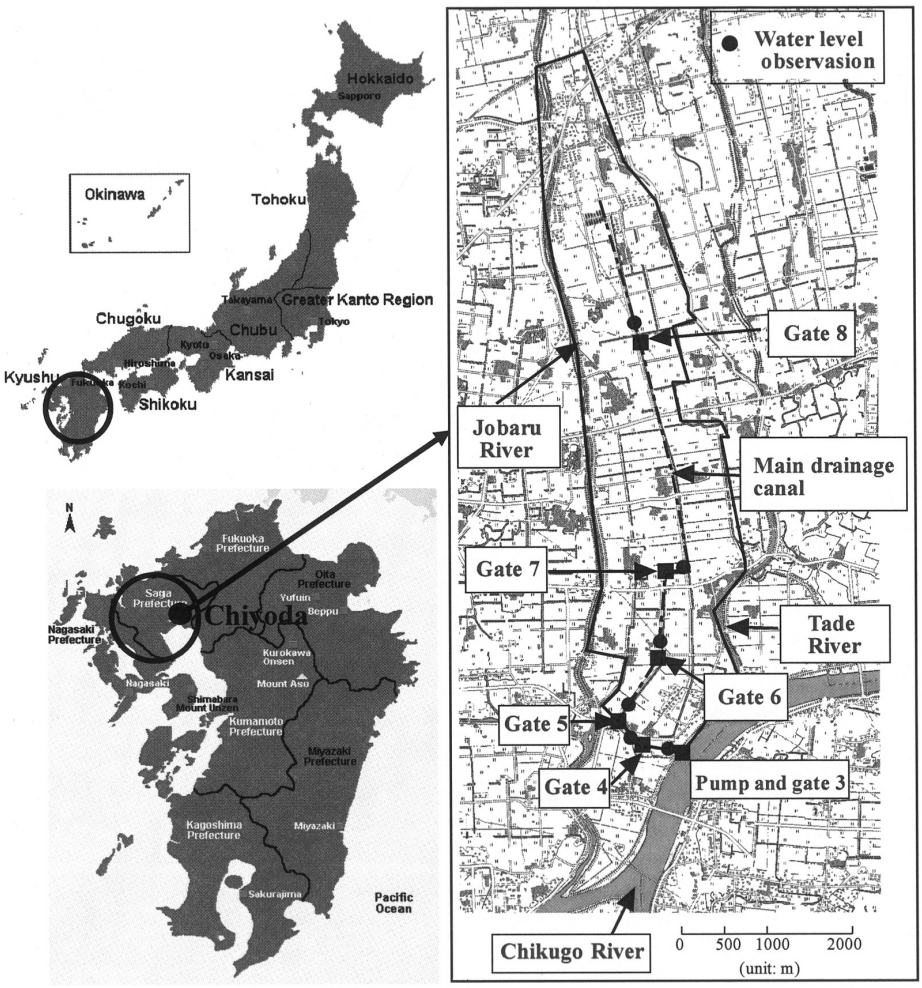

Fig. 1. Location of Chiyoda basin.

during flood events is removed from the paddy fields to secondary drainage canals, and then from the secondary canals to a main drainage canal, which has a length of 7.2 km. Finally, the excess water is discharged from the main drainage canal to the tidal compartment of the Chikugo River through gate and pumped drainage. All canals are used for both irrigation and drainage purposes.

In order to evaluate the applicability of the proposed model in the present study, water levels have been observed at the upstream of check gates by setting up the water level sensors from June 2005 and the water level data from June 23–26, 2006, were used for the verification of the proposed model. The water levels at the Chikugo River were also observed and used as the downstream boundary condition of the model. These observation points are shown in **Fig. 1**.

Modeling of the drainage system in Chiyoda basin

The models for drainage and inundation analysis in flat, low–lying paddy–cultivated areas are generally constructed based on the purposes of analysis and the characteristics of the drainage basin together with other related factors. Considering the characteristics of Chiyoda basin and the purpose of this study, a continuous tank model (Hiramatsu *et al.*, 2004) was adopted because it has a simple model structure and high performance. In the authors' model, the paddy fields and adjacent small canals were divided into "paddy tanks", and canals were divided into segments called "river tanks". Connecting the paddy tanks and the river tanks to each other, the flow discharge and direction at each connection branch were calculated by hydraulic equations using the differences between water levels in the tanks at both ends of the branch.

By dividing paddy fields and canals into paddy tanks and river tanks based on the topography and land use, the drainage network model of Chiyoda basin was obtained, as depicted in **Fig. 2**. The water level observation points are also shown in **Fig. 2**. The basin was analyzed by this model in which the paddy fields were divided into 14 tanks, the secondary drainage canals were divided into 10 river tanks, and the main drainage canal was divided into 14 river tanks. Therefore, there were 24 river tanks in total. The interfaces between the paddy tanks and the river tanks are drainage structures: 21 outlets from paddy fields to drainage canals or rivers, 8 sluice gates from the secondary drainage canals to the main drainage canal, 5 main check gates located in the main drainage canal, 1 gate, 1 pump and 1 flap gate located at the downstream end. The longitudinal section of the main drainage canal is depicted in **Fig. 3**. In

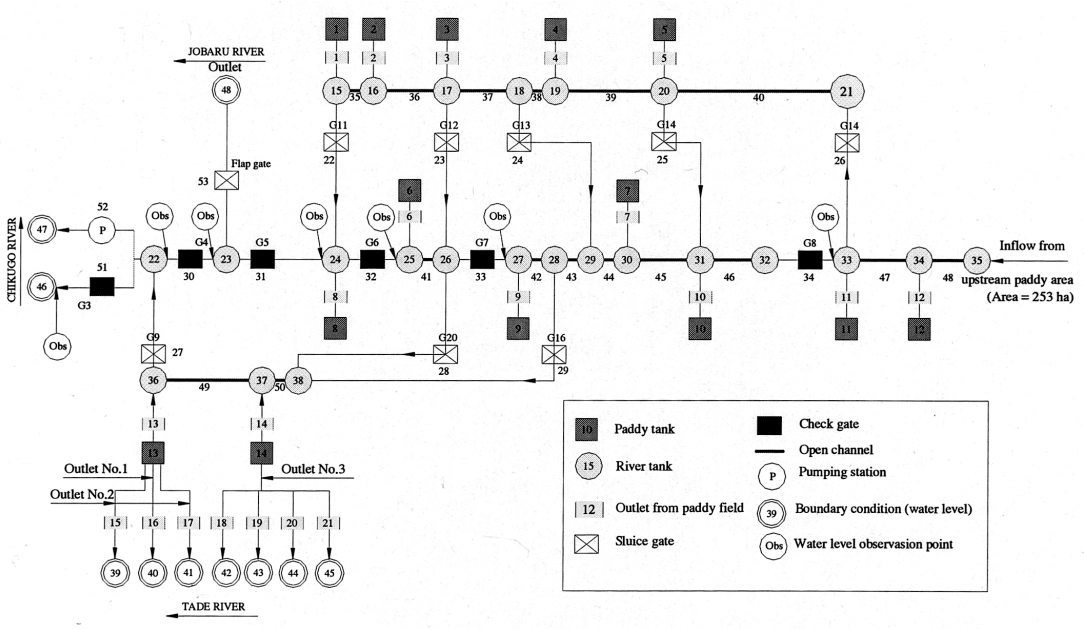

Fig. 2. Drainage network model of Chiyoda basin.

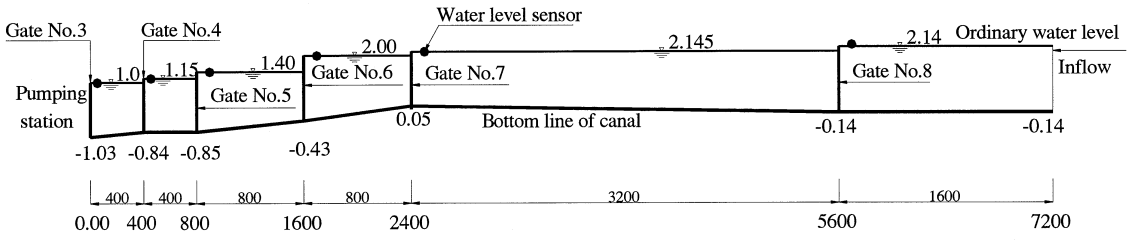

Fig. 3. Longitudinal section of Chiyoda drainage canal (unit: m).

order to meet the irrigation requirement during the irrigation period, the heights of the check gates are maintained at the ordinary water level for irrigation, which is the initial water level in numerical calculations.

Determination of water level and flow rate

This model was numerically solved to determine the water levels in the paddy tanks and the river tanks, and the flow discharges at every connection branch.

Assuming that the water level in each tank is uniformly varied, the variation of the water volume $V_{(i)}$ in tank i is described by the following continuity equation, which is a basis equation for calculating the flood inundation.

$$\frac{dV_{(i)}}{dt} = Q_{in(i)} - Q_{out(i)} \quad (1)$$

In equation (1), $V_{(i)}$, $Q_{in(i)}$ and $Q_{out(i)}$ are a water volume, an inflow to tank No. i and an outflow from tank No. i, respectively. The drainage network model in Chiyoda basin had 38 tanks, resulting in the simultaneous first–order ordinary differential equations with 38 unknown variables. These equations were numerically calculated by the Runge–Kutta–Gill method with a time step size of 10s. The flow rate Q at each connection branch was calculated by hydraulic equations using the differences between water levels in the tanks at both ends of the branch. Weirs, gates and open channels were assumed for hydraulic treatment of the connection branch, as shown in **Fig. 2**.

Calculation of flow rate

The dimensions of the paddy tanks, the river tanks, the paddy outlets, the sluice gates, the check gates and open channels are summarized in **Tables 1, 2, 3, 4, 5,** and **6**.

1) Paddy tank

If one paddy tank would consist of one paddy plot, there existed many paddy tanks in the basin model, which results in much calculation time. Therefore, the

Table 1. Dimensions of the paddy tanks (see also **Fig. 2**)

Tank number	Initial water level (lowest elevation) (m)	Area (m^2)	Tank number	Initial water level (lowest elevation) (m)	Area (m^2)
1	1.70	216,000	8	1.30	a643,000
2	2.00	344,000	9	2.10	1,017,000
3	2.20	486,000	10	2.10	683,000
4	2.20	340,000	11	1.80	999,000
5	2.00	442,000	12	1.70	866,000
6	1.60	490,000	13	0.90	688,000
7	2.10	927,000	14	1.60	312,000

Table 2. Dimensions of the river tanks (see also **Fig. 2**)

Tank number	Initial water level (m)	Elevation of bottom at the downstream end (m)	Area (m^2)	Length (m)	Bottom width (m)
15	1.700	−0.570	8,000	400	8.000
16	1.785	−0.480	8,000	400	8.000
17	2.038	0.010	24,000	1,200	8.000
18	2.123	0.220	8,000	400	8.000
19	2.292	0.270	16,000	800	8.000
20	2.545	0.360	24,000	1,200	8.000
21	2.545	0.360	16,000	800	8.000
22	1.000	−1.030	7,600	400	7.500
23	1.157	−0.840	4,600	400	8.500
24	1.400	−0.850	20,800	400	14.000
25	2.000	−0.430	10,400	800	14.000
26	2.000	0.050	10,400	400	14.000
27	2.145	0.120	10,400	400	14.000
28	2.145	0.170	10,400	400	14.000
29	2.145	0.210	10,400	400	14.000
30	2.145	0.250	10,400	400	14.000
31	2.145	0.290	20,800	400	14.000
32	2.145	−0.140	20,800	800	12.000
33	2.310	−0.140	10,400	400	12.000
34	2.310	−0.140	20,800	800	12.000
35	2.310	0.140	10,400	400	12.000
36	1.004	−0.570	8,000	400	8.000
37	1.316	−0.450	24,000	1,200	8.000
38	1.420	−0.050	8,000	400	8.000

Table 3. Dimensions of the paddy outlets (see also **Fig. 2**)

Outlet number	Width (m)	Bottom elevation (m)	Height (m)	Outlet Number	Width (m)	Bottom elevation (m)	Height (m)
1	3.000	1.700	1.000	12	11.000	1.700	1.000
2	5.000	2.000	1.000	13	9.000	0.900	1.000
3	7.000	2.200	1.000	14	4.000	1.600	1.000
4	5.000	2.200	1.000	15	0.890	0.490	1.000
5	6.000	2.000	1.000	16	1.400	0.950	1.000
6	7.000	1.600	1.000	17	1.000	0.490	1.100
7	12.00	2.100	1.000	18	4.000	1.360	1.500
8	8.000	1.300	1.000	19	4.500	−0.071	2.250
9	14.000	2.100	1.000	20	0.530	2.710	0.530
10	9.000	2.100	1.000	21	1.000	0.460	1.000
11	13.000	1.800	1.000				

Table 4. Dimensions of the sluice gates (see also **Fig. 2**)

Sluice gate number	Width (m)	Crest elevation (m)	Height (m)	WL_2 (m)
22	4.000	0.520	2.000	2.520
23	2.000	0.600	2.000	2.600
24	2.000	0.072	2.000	1.720
25	1.500	1.360	1.800	2.360
26	2.000	0.360	1.800	2.120
27	2.000	−0.070	3.800	0.930
28	4.000	1.100	2.000	2.100
29	4.000	0.180	2.000	3.080

Table 5. Dimensions of the check gates (see also **Fig. 2**)

Gate number	Width (Left) (m)	Width (Right) (m)	Bottom El. (m)	Crest height of weir (m)	D_{max} (m)	WL_1 (m)	$WL_{2(0)}$ (m)	$WL_{3(0)}$ (m)
30 (G4)	5.000	5.000	−0.843	1.157	3.750	1.407	1.807	2.807
31 (G5)	5.750	5.750	−0.600	1.400	3.500	1.500	1.900	2.800
32 (G6)	8.000	8.000	0.000	2.000	1.700	1.700	2.200	3.400
33 (G7)	5.000	10.000	0.145	2.145	3.300	2.345	2.845	3.345
34 (G8)	5.000	5.000	0.360	2.310	1.700	2.310	2.510	3.210

Table 6. Dimensions of the open channels (see also **Fig. 2**)

Open channel number	Width (m)	Manning's coefficient	Channel length (m)
35	8.000	0.020	400
36	8.000	0.020	800
37	8.000	0.020	800
38	8.000	0.020	400
39	8.000	0.020	1,000
40	8.000	0.020	1,000
41	14.000	0.020	400
42	14.000	0.020	400
43	14.000	0.020	400
44	14.000	0.020	400
45	14.000	0.020	600
46	12.000	0.020	800
47	12.000	0.020	600
48	12.000	0.020	600
49	8.000	0.020	800
50	8.000	0.020	800

present study assumed that one paddy tank consisted of several paddy plots and adjacent small canals, and introduced the conceptual and convenient modeling shown in **Fig. 4**. The relationship between the calculated water level and the inundation area in a paddy tank was identified by the preliminarily prepared relationship between the water level and the water surface area in the paddy tank.

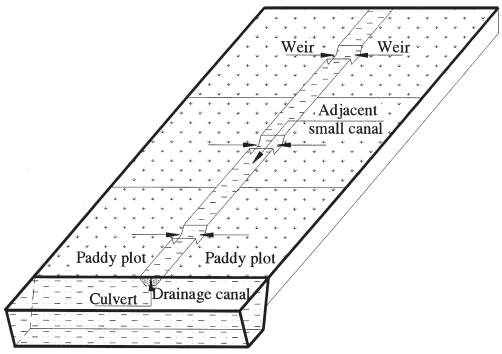

Fig. 4. Conceptual modeling of interface between paddy plots and a paddy tank.

The inflow rate from a paddy plot into a paddy tank was determined by the following equation:

$$\text{Inflow rate} = A_{(i)} \times Q_s \tag{2}$$

where $A_{(i)}$ is a total area of paddy plots included in the paddy tank No. i, and Q_s is the specific discharge from the paddy plots to the paddy tank through the outlets of paddy plots. The specific discharge Q_s, which results from the rainfall input to the paddy plot, was calculated by weir formula that corresponds to the critical flow as follows:

$$Q_s = 1.5495 B h_1^{3/2} \tag{3}$$

where B is a width of paddy plot outlet ($B = 0.83$ m/ha) and h_1 represents a overflow water depth on the outlet weir in the paddy plot. The excess water in the paddy tank was drained through a culvert, as shown in **Fig. 5**.

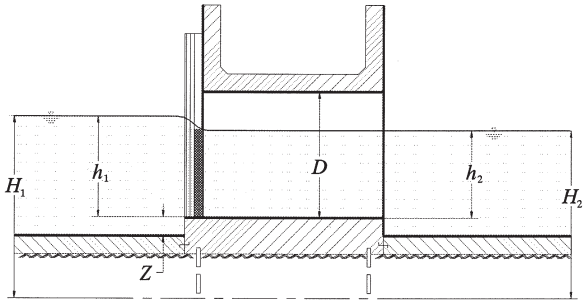

Fig. 5 Cross–section of check gate.

2) Rainfall input to river tanks

Rainfall input rate into the river tanks was determined by the following equation:

$$\text{Input rate} = A_{(i)} \times R \tag{4}$$

where $A_{(i)}$ and R are an area of river tank No.i and the rainfall intensity, respectively.

3) Hydraulic treatment: Culvert (Fig. 5)

In case of a paddy outlet or a sluice gate, the flow rate Q was calculated by the following equations:

a) Occupied flow: $h_1 \geq D$

– Critical flow: $h_2 \leq 2h_1/3$

$$Q = 0.635 BD \sqrt{2g(H_1 - 0.635D)} \tag{5}$$

– Submerged flow: $h_2 > 2h_1/3$

$$Q = 0.635 BD \sqrt{2g(H_1 - H_2)} \tag{6}$$

b) Not occupied flow: $h_1 < D$

– Critical flow: $h_2 \leq 2h_1/3$

$$Q = 1.5495 B h_1^{3/2} \tag{7}$$

– Submerged flow: $h_2 > 2h_1/3$

$$Q = 4.0258 B h_2 \sqrt{h_1 - h_2} \tag{8}$$

Here B is a width of outlet, D is a height of outlet, h_1 and h_2 represent water depths in the upstream and the downstream tanks above the bottom elevation Z of the outlet: $h_1 = H_1 - Z$, $h_2 = H_2 - Z$. The parameter g is a gravity acceleration.

4) Hydraulic treatment: Weir (Fig. 6)

The flow rate Q of weirs was calculated by the following equations:

a) Critical flow: $h_2 \leq 2h_1/3$

$$Q = 1.5495 B h_1^{3/2} \tag{9}$$

b) Submerged flow: $h_2 > 2h_1/3$

$$Q = 4.0258 B h_2 \sqrt{h_1 - h_2} \tag{10}$$

Here B is a width of weir, h_1 and h_2 are water depths in the upstream and the downstream tanks above the crest Z of bottom elevation of the weir: $h_1 = H_1 - Z$, $h_2 = H_2 - Z$.

In the case of a check gate or a gate, the operation is a combination of a weir and a culvert. Therefore, the flow rate Q of the check gate or gate was determined by the formula of a weir and a culvert.

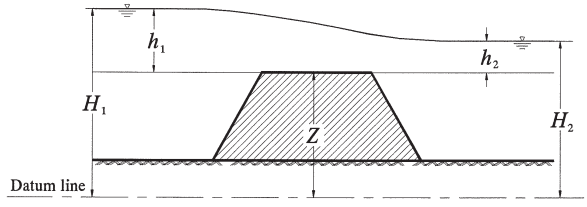

Fig. 6. Cross–section of weir.

5) Hydraulic treatment: Open channel (Fig. 7)

The flow rate Q was estimated by using Manning's formula (Chow, 1986) and the water level gradient S_0 between two river tanks:

$$Q = \frac{1}{n} A R^{2/3} \sqrt{S_0} \tag{11}$$

where A, R, S_0 and n represent a cross–sectional area, a hydraulic radius, a gradient and Manning's coefficient of

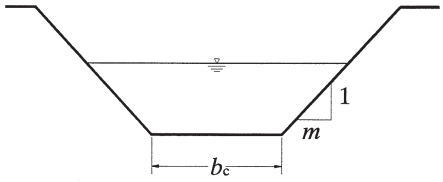

Fig. 7. Cross–section of open channel.

roughness. These parameters are calculated by the following equations:

$$A=\frac{1}{2}\left\{b_c+(b_c+2\times\frac{h_1+h_2}{2}\times m)\right\}\times\frac{h_1+h_2}{2};$$

$$P=b_c+2\sqrt{1+m^2}\times\frac{h_1+h_2}{2};\quad R=\frac{A}{P}$$

$$S_0=\frac{H_1+H_2}{L};\quad h_1=H_1-z_1;\quad h_2=H_2-z_2$$

where H_1, z_1, H_2, z_2 and b_c are water levels and bottom elevations at the upstream and the downstream of an open channel, and a bottom width. The parameters L and m are a length and a side slope of an open channel. The parameter m is a constant ($m=2.0$) in this basin.

6) Hydraulic treatment: Flap gate (Fig. 8)

In the case of a flap gate, the flow rate Q was determined by the following equations:

(a) Full occupied: $H \geq d_a$

$$Q=yBd_a\sqrt{2g\delta} \tag{12}$$

If $x \geq 0.88$ then $y=1.02$; If $x<0.88$ then $y=1.02-2.42\,(0.88-x)^3$,

where $x=3\sqrt{H_e\,\delta}/D_a$; $H_e>D_a \Rightarrow H_e=D_a$

(b) Sub–critical: $d_a>H>2H_e/3$

$$Q=yBH\sqrt{2g\delta} \tag{13}$$

If $x \geq 0.88$ then $y=0.98$;

If $x<0.88$ then $y=0.98-3.41(0.8-x)^3$, where

$x=3\sqrt{H_e\,\delta/D_a}$;

$H_e>D_a \Rightarrow H_e=D_a$

(c) Critical: $H \leq 2H_e/3$

$$Q=1.7yBHe^{3/2} \tag{14}$$

If $H_e>0.2\,D_a$ then $y=0.88\sim0.94$;

If $H_e \leq 0.2\,D_a$ then $y=0.98-3.41(0.8-x)^3 \leq 0.88$,

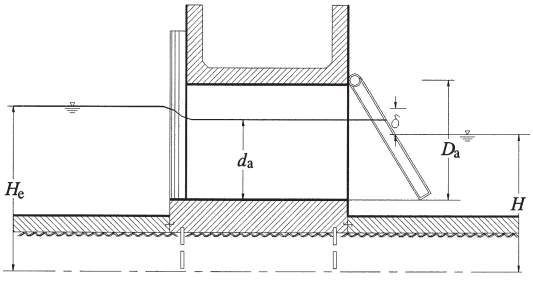

Fig. 8. Cross–section of flap gate.

where $x=1.732H_e/D_a$, B and D_a are the width and the height of the flap gate, H_e and H are the water head at the upstream and the downstream, δ is the difference of the water head between the upstream and the downstream. The parameters of B and D_a of the flap gate at the downstream end are $B=4.0$ m, $D_a=2.0$ m.

Gate operation

The most important point in the simulation of gate operation is that the operation process in the simulation model should be based on the actual gate operators' experiences. By investigating the actual conditions in Chiyoda basin and referring to the operators' experiences, it was assumed in the simulation model that the water levels at the upstream and the downstream of a gate are checked by a gate operator at two–hour intervals. Depending on the water levels checked during every two–hour interval, if necessary, the closing or opening operation of the gate was executed with a gate moving speed of 0.1 m per 10 s.

In the gate operation procedure, three water levels of WL_1, WL_2 and WL_3 play an important role. The water level WL_1 in the upstream of a check gate, which is an ordinary water level, meets the requirement for irrigation. The water level WL_2 at the upstream of a check gate is a water level at which the gate operation starts during flood events. The water level WL_3 at the downstream of a check gate is a water level at which the gate is closed in order to prevent the local concentration of excess water in the downstream area.

The outlets at the paddy tanks are fully opened during rainfall periods. Therefore, depending on the water levels in paddy tanks and river tanks, the flow direction sometimes changes to invert flow. The sluice gates located at the interface between the secondary drainage canal and the main drainage canal start to operate whenever the water level at the secondary drainage canal is higher than WL_2. At that time the sluice gates are fully opened.

The operation algorithm of check gates is depicted in **Fig. 9** and a flow diagram of the gate operation is shown in **Fig. 10**. When the water level at the upstream side (WL_u) of a check gate is lower than WL_1 before and after flood events, both right and left gates are closed and the weir remains at an elevation of WL_1 in order to store the water volume for irrigation purposes (**Fig. 9a**). When the water level at the upstream side (WL_u) of a check gate is higher than WL_2, the check gate begins to be operated. For the check gates No. 4, 5, and 7, the weir in the left side is lowered down until the minimum elevation (**Fig. 9b**), then the right gate is raised up (**Fig. 9c** and **Fig. 9d**), and finally the left gate is raised up (**Fig. 9e**). For the check gates No. 6 and 8, both right and left gates are raised up simultaneously. In order to prevent the local concentration of excess water in the downstream area, whenever the water level at the downstream (WL_d) of the check gates is higher than WL_3, both right and left gates are closed, and weir remains at the minimum elevation (**Fig. 9f**).

Gate No. 3, located at the downstream end adjacent

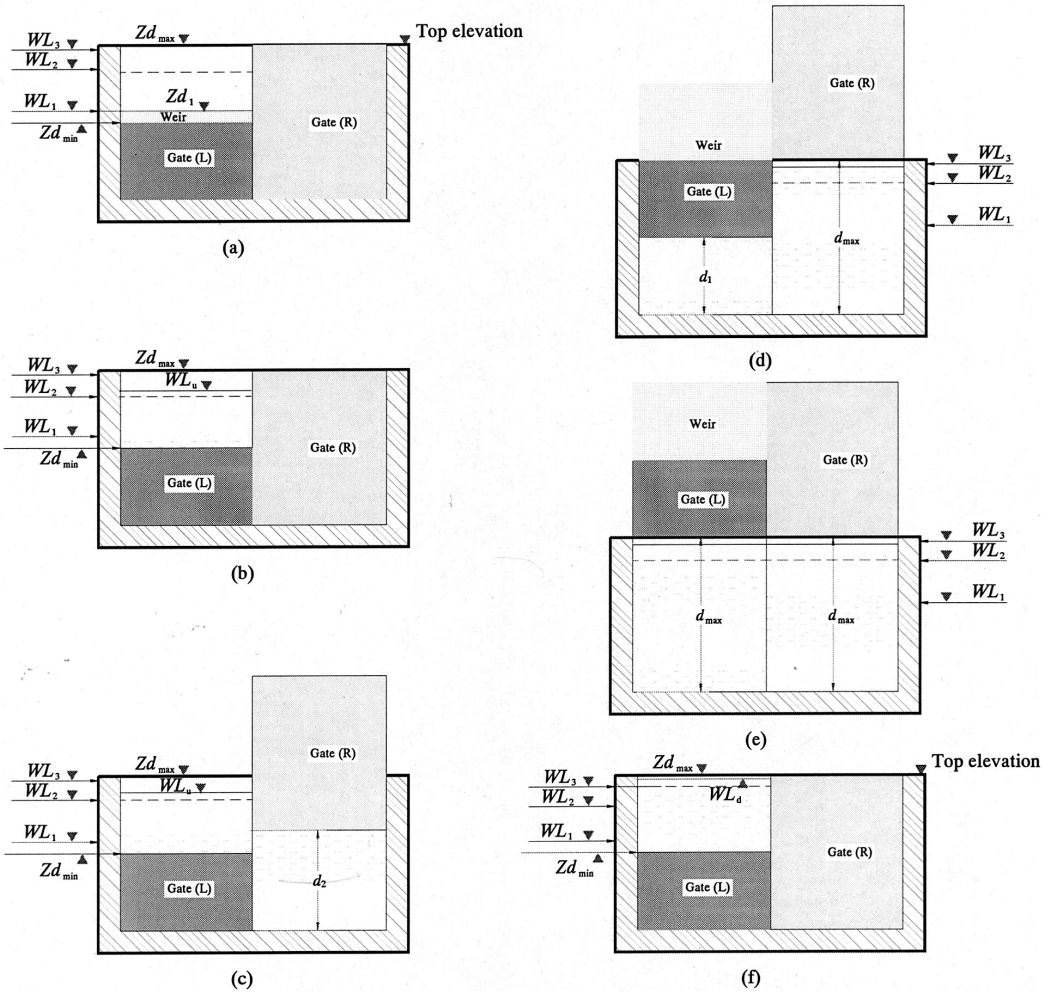

Fig. 9. Procesure of gate operation.

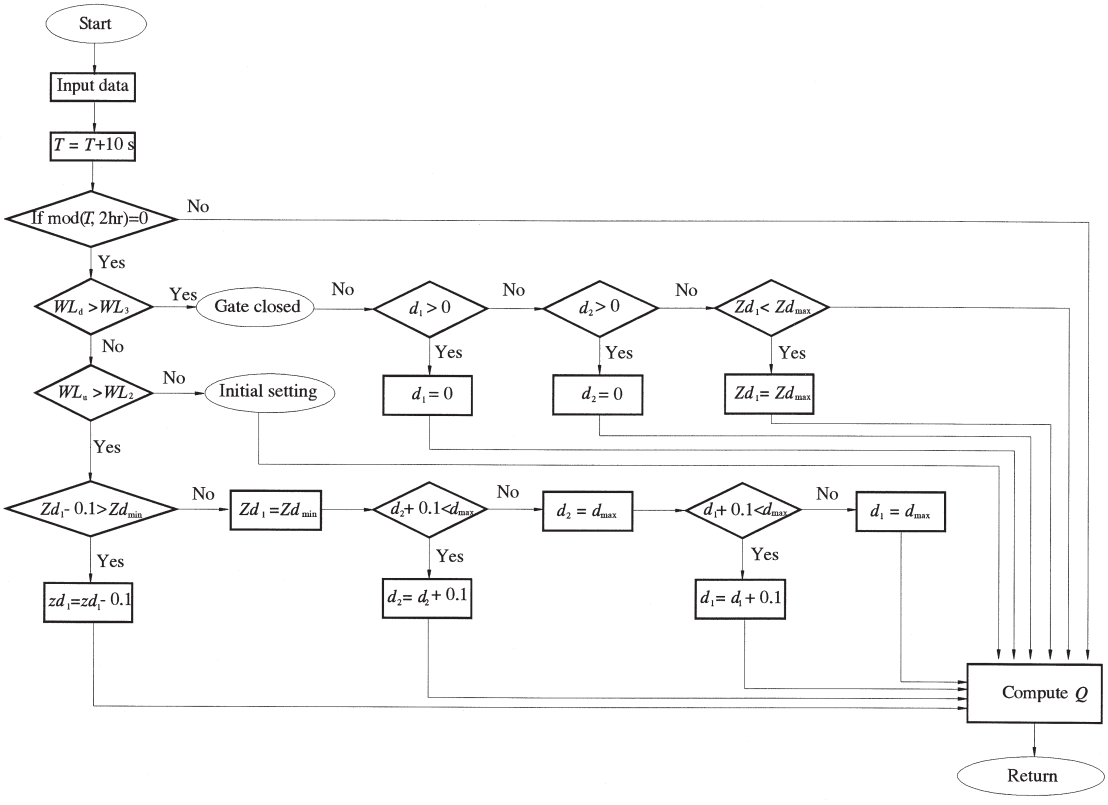

Fig. 10. Flow diagram of gate operation (see also **Fig. 9**).

to the Chikugo River, is fully opened whenever the water at the upstream main drainage canal is higher than both WL_a (WL_a=1.0 m) and the water level at the Chikugo River. The pump installed in parallel with gate No. 3 also starts to operate when the water level at the upstream main drainage canal is higher than H_p (H_p= 1.8 m).

Inundation scenario

After checking the accuracy of the model, the inundation parameters such as total inundation time, total inundation area, maximum water depth in paddy tanks were calculated using an stochastic rainfall time series with a return period of 30 years and the downstream boundary conditions of neap and spring tides in the Chikugo River.

The downstream boundary conditions

The water level in the Chikugo River that is affected by the variation of tide has been observed by a water sensor downstream of the check gate No. 3. Unfortunately, there was no observed water level data at the Tada River and the Jobaru River, while there are three outlets along the Tade River and one outlet along the Jobaru River, as shown in **Fig. 2**. Because these outlets are located at the upstream of intersections of the Chikugo River and the Tade River or the Jobaru River, the water levels at the outlets are affected by the variation of tide in the Chikugo River. Therefore, the water levels at the outlets, which were used as the boundary condition in the numerical simulations, were predicted based on the relationship between the observed water levels in the Chikugo River and the simulated water levels in the Tade River or the Jobaru River that are calculated by using one–dimensional continuity and momentum equations and the observed water levels in the Chikugo River as the downstream boundary condition. **Figure 11** depicts the relationship

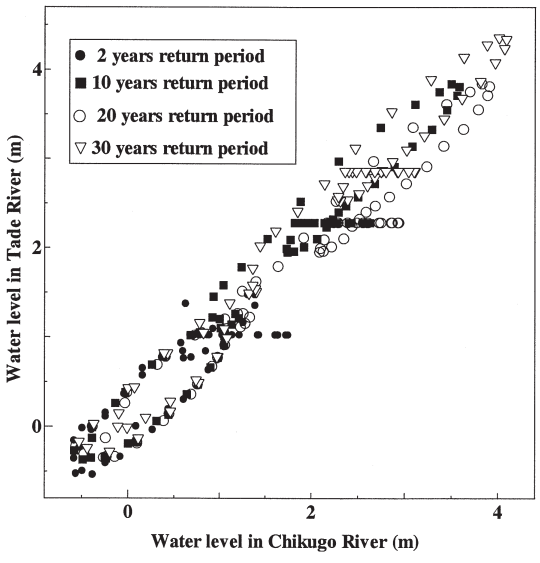

Fig. 11. Relationship between the water levels in the Chikugo River and the Tade River.

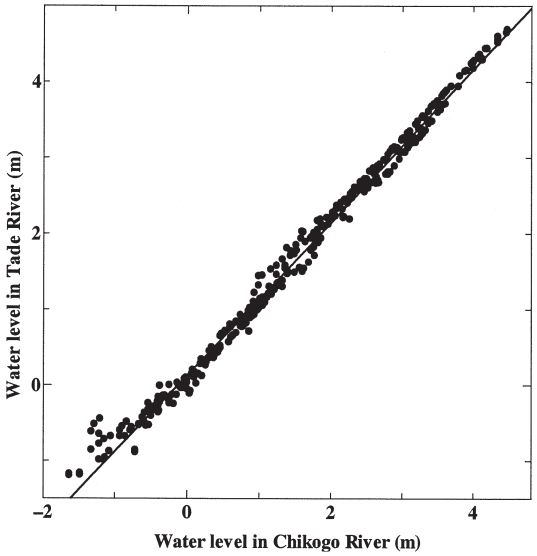

Fig. 12. Relationship between the water levels in the Chikugo River and the Tade River after adjusting the time delay due to tidal wave propagation.

between the observed water levels in the Chikugo River at time t and the simulated ones in the Tada River at time t. In this figure, the relation shows a characteristic and elliptical shape depending on the return periods. **Figure 12** shows the relationship after introducing a lag time by considering the time delay due to tidal wave propagation. The relationship was able to be approximated by the following linear functions.

At outlet No. 1 in the Tade River:

$$T_{1(t)}=0.03+C_{(t)} \quad (15)$$

At outlet No. 2 in the Tade River:

$$T_{2(t)}=0.08+C_{(t-1)} \quad (16)$$

At outlet No. 3 in the Tade River:

$$T_{3(t)}=0.13+C_{(t-1)} \quad (17)$$

At outlet in the Jobaru River:

$$J_{(t)}=0.5+C_{(t)} \quad (18)$$

where $T_{1(t)}$, $T_{2(t)}$, $T_{3(t)}$ and $J_{(t)}$ are the water levels at the outlets No. 1, No. 2, and No. 3 in the Tade River and the Jobaru River at time t. The variables $C_{(t)}$ and $C_{(t-1)}$ are the water levels in the Chikugo River at time t and (t – 1 hour). In the numerical simulations, these relations were used as the boundary condition.

Meteorological data

The ten–minute interval rainfall time series observed from June 23–26, 2006 (**Fig. 13a**), were used in the verification of the predicted performance of the Chiyoda drainage basin model. After the verification, the optimal gate operation that fully met both the flood drainage and the irrigation requirements were investigated using a stochastic rainfall time series with a return period of 30 years. The stochastic rainfall time series was determined from the observed data at Saga Local Meteorological Observatory from 1926 to 1996 by the Iwai method. The adopted three–day stochastic rainfall time series is depicted in **Fig. 13b**. A stochastic rainfall

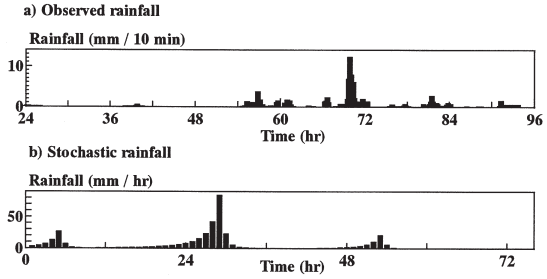

Fig. 13. Three–day rainfall.

time series with a return period of 10 years is adopted in the projects that have been carried out in this area by the Ministry of Agriculture, Forestry and Fisheries of Japan.

Evapotranspiration was not considered in the simulations. The vertical percolation was also not incorporated in the model because subsurface drainage due to percolation does not contribute to the removal of excess water during flood events in the study area.

RESULTS AND DISCUSSION

Applicability of the model

First, the accuracy of the proposed model was evaluated by comparing the simulated results with the observed water levels. In this simulation, the algorithm of gate operation shown in **Figs. 9** and **10** was used as the actual operation based on the operators' experiences, and the water levels of WL_2, WL_3 for the operation

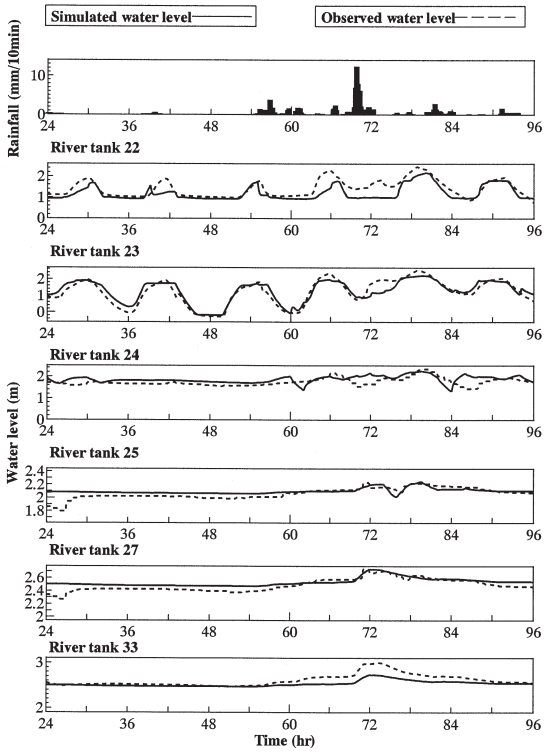

Fig. 14. Comparison of simulated results and observed water levels.

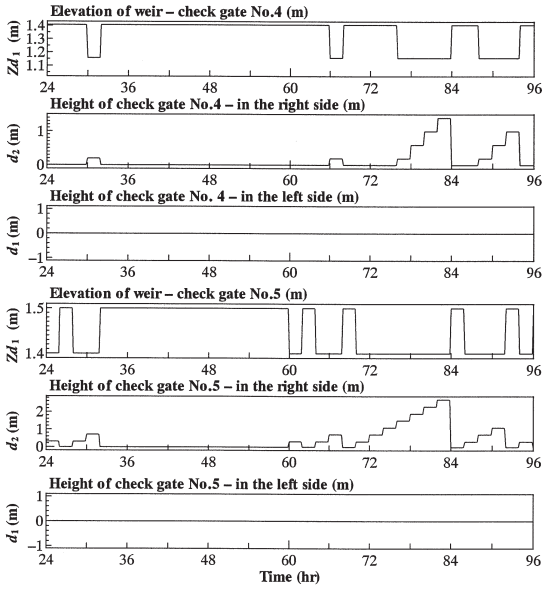

Fig. 15. Simulated results of gate operation process of check gates No. 4 and 5 (see also **Fig. 9** and **10**).

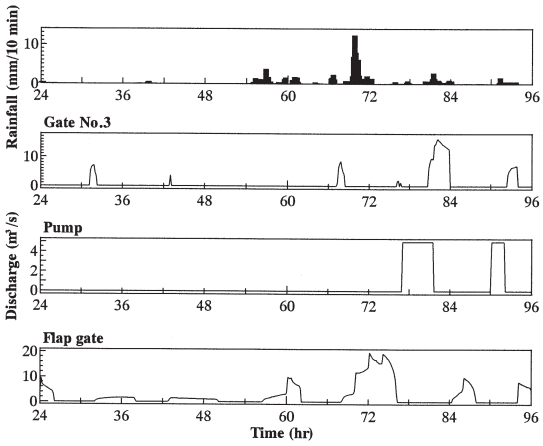

Fig. 16. Discharge of gate No. 3, pump, and flap gate at the downstream end.

were the same as the reference water levels of $WL_{2(0)}$ and $WL_{3(0)}$ shown in **Table 5**. Every gate was operated with a moving speed of 0.1 m per 10 s after checking the water levels at the upstream and the downstream of the check gate in two–hour intervals. The variation of water levels in river tanks 22, 23, 24, 25, 27, and 33 are shown in **Fig. 14**. The simulated operations of check gates No. 4 and No. 5, and the discharges at the downstream ends are depicted in **Figs. 15** and **16**, respectively. These figures show that the observed and simulated data are in good agreement. It was concluded that the Chiyoda basin model was successfully constructed by using a continuous tank modeling and the operation of check gates were well simulated by the algorithm defined in **Figs. 9** and **10**.

Second, the simulations were executed using a stochastic rainfall time series with a return period of 30 years incorporated with tidal conditions of both neap and spring tides in the Chikugo River. The inundation

Table 7. Total inundation time, total inundation area, and coefficient of variance of excess water depth in paddy tank in the simulations using a stochastic rainfall time series with a return period of 30 years incoporated with spring tide and neap tide in the Chikugo River

Tide type	Spring	Neap
Inundation time (hr)	406	324
Inundation area ($\times 10^6 m^2$)	2.24	2.20
Coefficient of variance	0.96	1.02

Table 8. Simulated results of maximum inundation depth in paddy tanks using a stochastic rainfall time series with a return period of 30 years incoporated with spring tide in the Chikugo River

Paddy tank numbe	Maximum Inundation depth (m)	Paddy tank number	Maximum Inundation depth (m)
1	0.46	8	0.85
2	0.16	9	0.05
3	−0.04	10	0.09
4	−0.04	11	0.55
5	0.16	12	0.66
6	0.56	13	1.24
7	0.10	14	0.54

Table 9. Simulated results of maximum inundation depth in paddy tanks using a stochastic rainfall time series with a return period of 30 years incoporated with neap tide in the Chikugo River

Paddy tank number	Maximum Inundation depth (m)	Paddy tank number	Maximum Inundation depth (m)
1	0.43	8	0.82
2	0.13	9	0.03
3	−0.07	10	0.07
4	−0.06	11	0.50
5	0.14	12	0.61
6	0.53	13	1.21
7	0.71	14	0.52

parameters such as a total inundation time, a total inundation area, a coefficient of variance of maximum inundation depth in paddy tanks, and maximum inundation depth in paddy tanks were calculated. In the analysis, the inundation in a paddy tank was defined as the situation in which a water level in the paddy tank is 0.05 m higher than the lowest elevation of the paddy tank. The total inundation time, the total inundation area, and the coefficient of variance of maximum inundation depth in paddy tanks are presented in **Tables 7**. **Tables 8** and **9** show the maximum inundation depth in the paddy tanks.

For futher study

The check gates play a very important role in the Chiyoda drainage system because they need to be controlled in order to minimize the damages for crop yield and to store irrigation water during and after flood events. Therefore, for further study, the check gate should be optimized in order to meet fully the said tagets. The optimal gate operation for both the drainage and the irrigation purposes can be investigated by trial and error method using a stochastic rainfall time series and the downstream boundary conditions of tides in the Chikugo River.

Conclusion

This paper presented a mathematical model of a drainage system in Chiyoda basin, which is a typical flat and low–lying paddy–cultivated area, for simulating the operation of gates in a main drainage canal and calculating the flood inundation. First, the algorithm of gate operation was simulated and the drainage model was then evaluated by comparing the simulated water levels with observed ones during an actual rainfall event. The results showed that the observed and simulated water levels were in good agreement, indicating that the proposed model was applicable for drainage and inundation analyses in flat, low–lying, paddy–cultivated areas. Second, the parameters of inundation scenario, which correspond to a stochastic rainfall time series with a return period of 30 years and the tidal conditions of spring and neap tides in the Chikugo River were predicted. A total inundation time, a total inundation area, a coefficient of inundation depth, and maximum inundation depth in paddy tanks were calculated. For further, this model will be able to provide managers and operators a usefull tool that is to optimize the gate operation in order to minimize the damages for crop and store the water for the irrigation purposes.

ACKNOWLEDGEMENTS

The authors wish to acknowledge the Chikugo River Basin Irrigation and Drainage Project Office, Kyushu Regional Agricultural Administration Office, the Ministry of Agriculture, Forestry and Fisheries of Japan for the acquisition of the measurement data of the water levels in the main drainage canal. We appreciate the helpful cooperation in modeling the drainage network in Chiyoda basin provided by Gijutsu Kaihatsu Consultant Co., Ltd., Fukuoka, Japan. Partial financial support for this study was provided by JSPS Grants–in–Aid for Scientific Research (B) (project number: 16380163 and 19380138). We would also like to thank all of the project members for their invaluable discussions.

REFERENCES

Bates, P. D. and A. P. J. De Roo 2000 A simple rates–based model for flood inundation simulation. *Jounal of Hydrology*, **236**: 54–77

Chen, R. S. and L. C. Pi 2004 Diffusive tank model application in rainfall–runoff analysis of upland fields in Taiwan. *Agricultural Water Management*, **70**: 39–50

Chen, R. S., L. C. Pi., Y. Huang 2003 Analysis of rainfall–runoff relation in paddy fields by diffusive tank model. *Hydrological processes*, **17**: 2541–2553

Chinh, L. V., K. Hiramatsu, M. Harada , M. Mori 2005 Optimal gate operation of a main drainage canal in a flat, low–lying

agricultural area using a tank model incorporated with a genetic algorithm. *Journal of Faculty of Agriculture Kyushu University*, **51(2)**: 351–359

Chow, V. T. 1986 *Open–channel Hydraulics*. McGraw–Hill Book Company, pp. 109–123

Dutta, D., S. Herath, K. Musiake 2006 An application of flood risk analysis system for impact analysis of a flood control plan in a river basin. *Hydrological processes*, **20**: 1365–1384

Durdu, O. F. 2006 Use Control of transient flow in irrigation canal using Lyapunov fuzzy filter–based. Gaussian regulator. *International journal for numerical methods in fluids*, **50**: 491–509

Ghumman, A. R., M. Z. Khan, M. J. Khan 2006 Use of numerical modelling for management o canal irrigation water. *Irrigation and drainage*, **55**: 445–458

Hiramatsu, K., S. Shikasho, K. Kurosawa, M. Mori 2004 Drainage and Inundation Analysis in a Flat, low–lying, Paddy–cultivated area of the Red River Delta of Vietnam. *Journal of Faculty of Agriculture Kyushu University* **49(2)**: 383–399

Horrit, M. S. and P. D. Bates 2001 Predicting floodplain inundation: raster–base modelling versus the finite–element approach. *Hydrological processes*, **15**: 825–842

Hsu, M. H., S. H. Chen, T. J. Chang 2000 Inundation simulation for urban drainage basin with storm sewer system. *Journal of Hydrology*, **234**: 21–37

Nicholas, A. P. and D. E. Walling 1997 Modelling flood hydraulics and overbank deposition on river floodplains. *Earth surface processes and landforms*, **22**: 59–77

Overton, I. C. 2005 Modelling floodplain inundation on a regulated river: Integrating GIS, remote sensing and hydrological models. *River research and application*, **21**: 991–1001

Pappenberger, F., K. Beven, M. Horritt, S. Blazkova 2005 Uncertainty in the calibration of effective roughness parameters in HEC–RAS using inundation and downstream level observations. *Journal of hydrology*, **302**: 46–69

Shikasho, S. and K. Tanaka 1985 Runoff Analysis of Low–lying Drainage Basins in Japan. *Irrigation Engineering and Rural Planning*, **8**: 5–17

Stewart, M. D., P. D. Bates, M. G. Andreson, D. A. Price, T. P. Burt 1999 Modelling floods in hydrologically complex lowland river reaches. *Journal of Hydrology*, **223**: 85–106